

A (1+1) dimensional example of Quarkyonic matter

Toru Kojo

*RIKEN BNL Research Center, Brookhaven National Laboratory,
Upton, NY-11973, USA*

Abstract

We analyze the (1+1) dimensional QCD (QCD_2) at finite density to consider a number of qualitative issues: confinement in dense quark matter, the chiral symmetry breaking near the Fermi surface, the relation between chiral spirals and quark number density, and a possibility of the spontaneous flavor symmetry breaking. We argue that while the free energy is dominated by perturbative quarks, confined excitations at zero density can persist up to high density. So quark matter in QCD_2 is an example of Quarkyonic matter. The non-Abelian bosonization and associated charge-flavor-color separation are mainly used in order to clarify basic structures of QCD_2 at finite density.

1 Introduction

The confinement is a distinct phenomenon in Quantum Chromodynamics (QCD). The confinement reveals its property in the physical spectra saturated by the color singlet states. Many features of spectra are qualitatively explained by the picture of the squeezed colored flux connecting colored objects.

Recently, the role of confinement in cold, dense quark matter has been addressed by McLerran and Pisarski [1]. They suggested that excitations can remain confined even after quarks are released from baryons to form quark matter. Such quark matter is named Quarkyonic matter [1,2,3,4], which is distinguished from the conventional quark matter with deconfined excitations. The understanding of excitation modes is important to consider the phase structure, transport phenomena, etc.

Before suggestions in Ref.[1], confining effects in quark matter have not been taken into account seriously. Presumably one of the reasons would be that

quarks seem to excite individually after being released from baryons. In addition, asymptotic freedom apparently implies that confining forces become irrelevant when the typical distance among quarks is very small.

In this paper, we are going to offer one counter example to such reasonings. While we expect that conventional reasonings work for most of regions in the quark Fermi sea, they do not reflect physics near the Fermi surface. To illustrate the points, we analyze QCD in (1+1) dimensions (QCD₂) as a theory with confining forces and asymptotic freedom [5,6,7,8,9,10]. We will conclude that cold, dense quark matter in QCD₂ is an example of Quarkyonic matter.

Our main statement is that the mechanism to suppress the confining gluons at finite density is neither asymptotic freedom nor the percolation of confined bags, but the medium induced color screening. Since the color charge of the system is zero in average, the strength of the screening is determined by the virtual processes. The main actors are the virtual colored fluctuations with low energy: quarks near the Fermi surface. The contributions from virtual quark fluctuations are enhanced as the area of the quark Fermi surface grows. In spatial dimensions, d , larger than one, the phase space for quark fluctuations increases as $\sim \mu^{d-1} \Lambda_{\text{QCD}}$, so the strength of the screening grows as $\sim (\mu/\Lambda_{\text{QCD}})^{d-1}$, compared to the vacuum case ($\mu, \Lambda_{\text{QCD}}$ are quark chemical potential and nonperturbative scale, respectively). So deconfinement should take place when quark fluctuations become comparable to those of gluons,

$$N_c \times (\mu/\Lambda_{\text{QCD}})^{d-1} \sim N_c^2 \longrightarrow \mu \sim N_c^{\frac{1}{d-1}} \Lambda_{\text{QCD}}, \quad (1)$$

where we have multiplied color factors for quarks, N_c and for gluons, N_c^2 . In our world, $d = 3$, so the gluon sector is modified at $\mu \sim N_c^{1/2} \Lambda_{\text{QCD}}$, as given in Ref. [1]. This is parametrically larger than the scale, $\mu \sim \Lambda_{\text{QCD}}$, where nuclear matter appears and shortly later turns into quark matter [1].

This picture for deconfinement at finite density implies that in spatial one dimension, *if* the excitations are confined at zero density¹, they must survive even at very high density, $\mu \gg \Lambda_{\text{QCD}}$, because the phase space for quark fluctuations remains the same as the vacuum case, and as a consequence, screening effects are not enhanced. We will check that this is indeed the case in our QCD₂ studies.

The second purpose of this paper is to examine mechanisms of the chiral symmetry breaking near the Fermi surface (modulo strong infrared phase fluctu-

¹ The analyses in this paper do not answer whether excitations are confined at zero density. In the large N_c limit, the theory is confining, at least in the presence of arbitrary small current quark mass [5]. On the other hand, in the large flavor limit such that $N_c/N_f \rightarrow 0$, it is argued that the color sector takes a similar form as the Schwinger model — Higgs phenomenon happens due to the screening [11].

ations peculiar to (1+1) dimensions [12,13,14]), which recently attract much attentions in (3+1) dimensional quark matter in the context of inhomogeneous chiral condensates [3,4,15,16,17,18,19]. We also study the relationship among quark density, chiral condensates, and a scale generated in the colored sector. In (1+1) dimensions, such a relationship can be seen at the operator level [20,21,22,23,24,25]. Such operator relations do not strictly hold in higher dimensions. But at high density such that the curvature of the Fermi surface is negligible, there emerge certain circumstances in which low dimensional picture of the Fermi surface is useful². The detailed understanding of QCD₂ would provide a useful way of thinking for these situations.

One of the most enlightening approaches to discuss the above issues in QCD₂ is the non-Abelian bosonization [21]³. The use of it is motivated by at least two reasons.

First, the bosonized form allows us direct access to the colorless objects such as quark number density or chiral density. A number of conclusions can be derived without explicitly treating the colored objects and confining interactions among them, which are not easy to deal with. This is not the case in usual fermionic expressions in which we have to built up color singlet quantities from quark propagators. The trouble is that even if we investigate a single quark propagator very precisely, its property can not be directly converted into physical quantities because residual confining interactions are so strong [6] — the physical interpretation of results may be done only after we construct colorless objects for which residual interactions are under control.

The second reason comes from utility of the charge-color separation, analogous to the spin-charge separation in the condensed matter system [23,24]. In chiral limit, the quark number and colored sectors decouple as [8,25]

$$S_{\text{fermion}} \longrightarrow S_{U(1)}[\varphi] + S_{\text{color}}[h], \quad (2)$$

so that bosonized fields responsible for $U(1)$ quark number (φ) and color densities (h) can be treated separately. It means that the color sector remains the same at any quark density, since quark chemical potential couples only to quark number density, not to color density. Hence confined excitations at zero density persist up to arbitrarily high density.

The charge-color separation is also useful to get insights of the chiral symmetry

² At high density, transverse dynamics along the Fermi surface provides negligible contributions, $\sim p_{\perp}^2/\mu$, to the energy spectra. This can be used to factorize integral equations such as the Schwinger-Dyson equation near the Fermi surface by *integrating out* transverse dynamics, instead of just ignoring it. The resulting equation is dimensionally reduced one. Such treatments are done in [3,4,15,16,17].

³ For other approaches based on the holography, see Ref. [26], for instance.

near the Fermi surface. In chiral limit, the chiral condensate in the bosonized form has the following factorized structure,

$$\langle \bar{\psi}_L \psi_R \rangle = \langle \text{tr} h \rangle \langle e^{i\varphi} \rangle. \quad (3)$$

Since $\langle \text{tr} h \rangle$ is unaffected by quark density, density effects appear only through the exponent $\langle e^{i\varphi} \rangle$. The color sector serves a massive scale for the amplitude of the chiral condensate, while the quark number sector provides a phase rotation. Through the operator relations, we will see a single baryon accompanies a single chiral spiral. Then it follows that at nearly uniform quark density, largely overlapped baryons, which are merged with other baryons, induce a lot of chiral spirals with period $\sim 1/2\mu$. This period reflects that the chiral condensates are made of co-moving particles and holes near the Fermi surface, with momenta $p_f \sim \mu$. Similar results have been found in other approaches [27,28]. We will also argue that chiral symmetry breaking effects are relevant near the Fermi surface, while not in most regions of the Fermi sea.

Throughout our discussions, we try to specify peculiarities in (1+1) dimensions as much as possible. Useful qualitative pictures applicable to (3+1) dimensions may emerge only after the identification of such (1+1) dimensional specialities.

This paper is organized as follows. In Sec.2, we give general remarks on the Fermi sea in Quarkyonic matter. Then QCD₂ is briefly discussed in the fermionic language. We will also explain why we think of the quark Fermi sea, instead of the baryonic Fermi sea. In Sec.3, the basics of the non-Abelian bosonization are quickly reviewed. In Sec.4, one baryon, two baryons, and finite baryon density are pedagogically discussed. The relationship between chiral spirals and baryons or quark number density is shown. In Sec.5, we argue the extension to two flavor case. In Sec.6, terms which enhance or suppress the formation of chiral spirals are classified. Sec.7 is devoted to the summary and discussions. Throughout this paper, we fix the value of $N_c g_s^2$ when we change N_c from three.

2 General remarks on the quark Fermi sea

Before performing explicit calculations, we argue qualitative aspects of the Fermi sea in Quarkyonic matter. To emphasize conceptual points, we first consider very high quark density, $\mu \gg \Lambda_{\text{QCD}}$, where the inter quark distance is much smaller than a typical distance scale of confinement. Baryons already overlap one another so that quarks need not belong to particular baryons. The lower density will be discussed later in order to emphasize how nuclear and Quarkyonic matter are related.

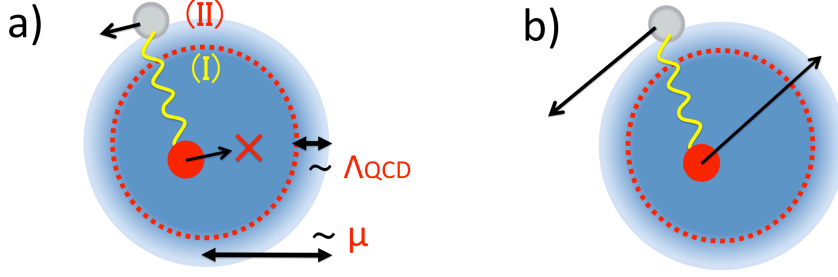


Fig. 1. The scattering of quarks in the region (I), $|\vec{p}| \lesssim \mu - \Lambda_{\text{QCD}}$. (a) Small momentum exchange processes, which are forbidden by Pauli blocking. (b) Hard momentum exchange processes, which transfer quarks from the region (I) to its outside. (Dotted lines separate the regions (I) and (II).)

Here we should specify our terminology used in this paper. The confinement and deconfinement will be classified by excitation modes. We think that this will give more precise classifications than those based on releasing of quarks from baryons. For example, the former distinguishes whether correlation functions for glueball operators contain deconfined multi-gluon spectra or not ⁴.

What are relationships between asymptotic freedom and quark density? When the inter quark distance is small, typical interactions are supposed to be weak because of asymptotic freedom. This logic is frequently used to justify weak coupling treatments of high density QCD as well as to guarantee the picture of the degenerated quark Fermi sea.

For more precise statements, we divide regions of the Fermi sea into (I) an inner region ($|\vec{p}| \lesssim \mu - \Lambda_{\text{QCD}}$) and (II) a surface region ($|\vec{p}| \gtrsim \mu - \Lambda_{\text{QCD}}$) (see Fig.1(a)). Let us clarify properties of interacting quarks in each region, by arguing possible corrections from virtual scattering processes.

In the region (I), Pauli principle prevents quarks from being scattered by small momentum exchanges (Fig.1(a)). Thus quarks in the region (I) have little chance to feel nonperturbative effects. Allowed processes are hard scatterings which transfer quarks to the outside of the Fermi sea (Fig.1(b)). The latter may be treated within weak coupling methods. Therefore quarks in the region (I) can be described by quasi-particles affected by perturbative self-interactions and many body effects.

⁴ We have to admit that practically it is not easy to make such a distinction in a solid way. For instance, in chiral limit and at zero density, the spectral function for the ρ meson channel contains the cut of multi-pions starting from zero invariant mass. On the other hand, we know that the height of multi-pion spectra of $O(N_c^0)$ is much lower than that expected from $q\bar{q}$ continuum of $O(N_c)$. So we can interpret this hierarchy as a consequence of confinement. Unfortunately this classification becomes again ambiguous in the quark-hadron duality region at high energy [29].

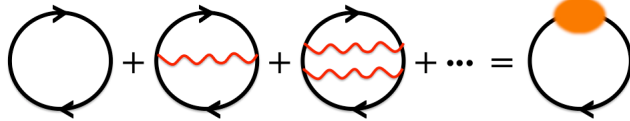


Fig. 2. A uncorrelated sum of the single quark loops. The Fock term is a part of the full quark propagator at large N_c .

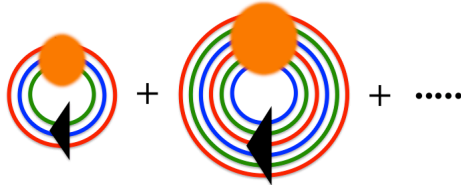


Fig. 3. A sum of the color singlet loops with $n \times N_c$ quarks, where n is an integer. The $N_c = 3$ case is shown. In the dilute regime, these diagrams can be factorized into a sum of baryon loops with a few number of the meson interactions. In the dense regime, the quark exchange frequently occurs, so we need more general descriptions than the baryonic matter.

The above argument is incomplete, since there are also contributions from zero momentum exchange processes, in which quarks just exchange positions in the Fermi sea (the Fock term, the second diagram in Fig.2). Thereby those processes are allowed inside of the Fermi sea, and should be sensitive to the gluon propagator at zero momentum. It would cause problems in computations of several quantities such as the total free energy. Such computations include quark loops which may contain virtual gluon loops with zero momentum transfer. For some gauge, gluon propagator shows divergent behavior in the deep IR region, so such diagrams would cause the IR divergence⁵.

If we compute the total free energy as an *uncorrelated* sum of the *single* quark loops (Fig.2), the deep IR behavior of gluon propagators is a certainly serious problem. However, in computations of the color singlet Fermi sea, it may be possible that the deep IR contributions cancel out after self-consistent treatments or resummation together with other quark loops. Such contributions can not be mimicked by an uncorrelated sum of single quark loops — we cannot derive any physical conclusions for color singlet objects until we correctly take into account the interactions among quark loops which make diagrams color singlet (Fig.3).

There is a case study for the $1/\vec{p}^4$ confining propagator in (3+1) dimensions. It indicates that the deep IR contributions at $\vec{p} = \vec{0}$ are canceled out after consistent treatments of the quark self-energy and confining interactions in

⁵ A similar problem has been discussed in case of an electron gas, and usually one handles this by including the Debye screening mass to kill the infrared divergences from photon propagators.

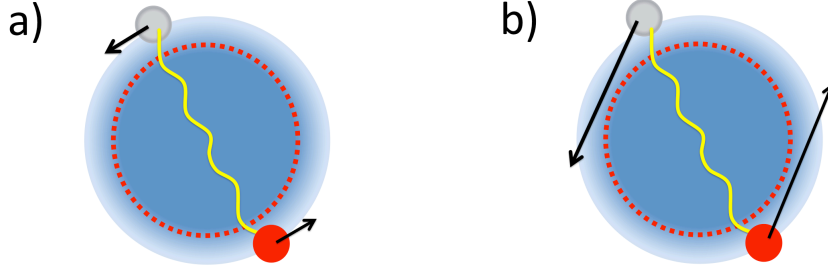


Fig. 4. The scattering of quarks in the region (II), $|\vec{p}| \gtrsim \mu - \Lambda_{\text{QCD}}$. (a) Small momentum exchange processes as sources of nonperturbative phenomena. (b) Hard momentum exchange processes. Both processes are allowed.

the color singlet objects⁶. Intuitively, this cancellation may reflect that the gluon propagator at $\vec{p} = \vec{0}$, which corresponds to an infinitely long string configuration⁷, can not be relevant inside of color singlet objects.

Although we are not aware of whether this cancellation generically holds in any confining models in (3+1) dimensions, we will rely on this qualitative interpretation for the nonperturbative part. In (1+1) dimensions, we will see that no problems arise from the confining force at finite density.

Now let us consider the region (II). There soft momentum exchanges (Fig.4.(a)) are allowed in the region (II). In addition to perturbative effects (Fig.4.(b)), nonperturbative effects on quarks also operate here, and properties of quarks near the Fermi surface may be strongly modified from those of quasi-free fermions.

With these pictures for quarks, let us first examine bulk thermodynamic quantities to which all quarks in the Fermi sea contribute. A schematic picture is given in Fig.5, taking the pressure as an example. At high density, they are well saturated by contributions from the region (I), simply because a number of quarks is much larger than those in the region (II). The region (I) gives contribution of $\sim \mu^4$ including perturbative corrections, while we get small (nonperturbative) contribution of $\sim \mu^2 \Lambda_{\text{QCD}}^2$ from the region (II). In this sense, the picture of perturbative quarks should work in computations of bulk quantities, and should reproduce perturbative results [31].

⁶ The simplest way to show the cancellation is to just use the principal value regulator for the $1/\vec{p}^4$ force for which the propagator takes zero value at $\vec{p} = \vec{0}$ [6]. In Ref.[30], usual IR cutoff scheme is used to argue the cancellation. While two schemes provide different quark propagators, they give the same spectra at the level of the Bethe-Salpeter equation. Thus the detail of $\vec{p} = \vec{0}$ is irrelevant as far as consistent calculations are performed.

⁷ In the usual IR cutoff scheme, $-\int d\vec{p} \frac{\sigma}{(\vec{p}^2 + \mu_R^2)^2} e^{i\vec{p} \cdot \vec{r}} \sim -\frac{\sigma}{\mu_R} e^{-\mu_R r} \sim -\frac{\sigma}{\mu_R} + \sigma r + O(\mu_R r^2)$, where μ_R is infinitesimal. The first term is independent of \vec{p} , and expresses a string with infinite length.

$$P = c[1 + c_1\alpha_s(\mu) + \dots]\mu^4 + O(\mu^2\Lambda_{\text{QCD}}^2)$$

• (I):

- Number of d.o.f. : **Large**
- Quark properties: **Perturbative**

• (II):

- Number of d.o.f. : **Small**
- Quark properties: **Non-perturbative**

Fig. 5. The pressure as an example of bulk quantities. The dominant contribution ($\sim \mu^4$) comes from the region (I) including a large number of (perturbative) quarks.

Again, we do *not* insist that the pressure in Quarkyonic matter can be computed from a sum of non-interacting single quark loops in a literally sense. Interacting diagrams, which include other quark lines in a color singlet way, must be included to avoid the problem of infinitely long strings generated from quarks. Our claim is that once this particular infrared problem is handled, quarks inside of the Fermi sea should look like perturbative quarks.

While the bulk quantities should be well-approximated by perturbative contributions, physics near the Fermi surface is sensitive to the excitation modes and nonperturbative effects. Examples are the phase structures, transport phenomena, etc. The issues of confinement and chiral symmetry breaking are nontrivial here.

To examine pictures discussed so far, let us take one flavor massless QCD₂ as an example. The action of QCD₂ with axial gauge fixing is

$$S = \int d^2x \bar{\psi}(x)(i\not{\partial} + \mu\gamma^0)\psi(x) + \int d^2x d^2y J_A^\mu(x) D_{\mu\nu}^{\text{AB}}(x-y) J_B^\nu(y), \quad (4)$$

where $x = (t, z)$, $J_A^\mu = \bar{\psi} t_A \gamma^\mu \psi$, and t_A is usual color matrix in the fundamental representation. Its normalization is $\text{tr}[t_A t_B] = \delta_{AB}/2$. The interactions between colored currents are confining, and instantaneous in axial gauge, $D_{\mu\nu}^{\text{AB}}(x-y) = \delta^{\text{AB}} \delta_{\mu 0} \delta_{\nu 0} |\vec{x} - \vec{y}|$. The gluon propagator is not dynamical in (1+1) dimensions, so we have eliminated the gluon fields using the equation of motion. Note that the gauge coupling constant has a dimension one, and serves the scale Λ_{QCD} in (1+1) dimensions.

In the presence of the Fermi sea, it is convenient to redefine quark fields depending on their moving directions $+z$ or $-z$,

$$\psi_\pm(t, z) = e^{\pm i\mu z} \psi'_\pm(t, z). \quad (5)$$

Its shorthand notation is $\psi = e^{i\mu\gamma_5 z}\psi'$, since eigenvalues of $\gamma_5 = \gamma_0\gamma_z$ coincide with moving directions in (1+1) dimensions,

$$\bar{\psi}i\partial\psi = \psi_-^\dagger i(\partial_0 + \partial_z)\psi_- + \psi_+^\dagger i(\partial_0 - \partial_z)\psi_+. \quad (6)$$

So Eq.(5) just means shifts of momenta to measure them from the Fermi surface, $\pm\mu$. With these new fields, we obtain

$$\bar{\psi}(x)(i\partial + \mu\gamma^0)\psi(x) \rightarrow \bar{\psi}'(x)i\partial\psi'(x), \quad J_A^\mu(x) \rightarrow (J'_A)^\mu(x), \quad (7)$$

and the Lagrangian becomes that of the zero density.

Since Lagrangian is the same as that in vacuum, properties of excitations such as energies are also unchanged except their shifted momenta. Therefore in (1+1) dimensions, if models have confined excitations in vacuum, they also do at finite density. This is true no matter how quark density is high and inter quark distances are short. The value of N_c is not essential in the present discussion. An overlap of baryons and deconfinement do not have one to one correspondence.

In coordinate space, this situation may be difficult to imagine if we view quarks as point-like particles as classical mechanics. Perhaps it is easier to understand if we see the distribution of colors by focusing on the wave properties of quarks. Closely packed quarks form a color singlet background minimizing the color charge in the system, and excitations are deviations from such a background. Quarks and quark-holes always appear together as confined excitations.

To what extent can we generalize these pictures to the higher dimensions? The main changes can be found in the phase space allowed for colored $q\bar{q}$ fluctuations which screen the exchange of gluons.

In (1+1) dimensions, phase space near the edge of occupied states are always the same in the Dirac and Fermi sea. Thus the strength always looks same in a whole density region. This explains why the excitation energy near the Fermi surface does not change even at asymptotically high density.

In spatial dimensions larger than one, the phase space for fluctuation modes increases as density does. Eventually interactions between colors are strongly screened, or squeezed color fluxes dissociate completely. Then weak coupling methods become enough to describe not only bulk quantities but also excitation modes.

Currently we have only a rough estimate of such density for the (3+1) dimensional system, $\mu \sim N_c^{1/2}\Lambda_{\text{QCD}}$, parametrically larger than density where baryons overlap, $\mu \sim \Lambda_{\text{QCD}}$. The relevance of the present discussions to (3+1) dimensions depends on how widely these two scales are separated after in-

cluding all other numerical factors. Attempts to estimate such a width can be found in several model studies [32,33,34].

So far we have considered only high density regime in which the concept of Quarkyonic matter is most clearly illustrated. Now let us consider how such high density regime is connected to lower density regime where the presence of nuclear matter is important.

Perhaps it is good to start with seeing how the picture of the baryonic Fermi sea in nuclear matter breaks down as density increases. The main problem is the difficulty to maintain the quasi-particle picture of baryons. Typical interactions among baryons get stronger at shorter distance, or in harder momentum transfer processes. This means that baryons near the Fermi surface and deeply inside of the Fermi sea can strongly affect one another. This badly destroys the concept of the baryonic Fermi sea at very high nuclear density⁸.

After all, at high density, we have no right to stick to the Fock space made of conventional baryons made of N_c quarks. The Fock space including baryonic objects made of $2N_c, 3N_c, \dots$ quarks, which are also color singlet, may become equally important (Fig. 3). This is so, because energetically such states may be easily reached by strong forces among ordinary baryons as well as by large collision rates at high baryon density. We will give more detailed arguments in Sec. 4.3.

This signals that effective degrees of freedom should be switched from baryons to quarks, in order to temper the growth of residual forces among the objects which we chose as basic degrees of freedom. At shorter distance, most of quarks feel weaker interactions, so they are reasonable alternatives forming the Fermi sea. Hence we expect that the transition from nuclear to Quarkyonic matter smoothly proceeds inside of the Fermi sea, while in both matters excitations remain confined.

Here we should stress again that the basic ingredients of the above arguments are properties of interactions – whether composite objects overlap or not, is the secondary issue. For instance, if the baryon based descriptions gave smaller corrections of interactions than those in quark descriptions, we could continue to use the picture of the baryonic Fermi sea even at very high density. Of course such a situation is very unlikely in QCD. Needless to say, knowledges about baryon-baryon interactions at high density are crucial for further arguments.

⁸ The reconstruction of the Fermi sea should happen at some density without depending on whether N_c is odd or even, or whether baryons are composite fermions or bosons. Even if baryons are composite bosons, we start to observe their internal structures made of fermions at density of the baryon overlap — the Pauli principle acts on the internal momenta of fermions.

In summary, Quarkyonic matter differs from conventional quark matter in the excitation modes, and should be distinguished from nuclear matter by bulk quantities.

3 The non-Abelian bosonization of QCD₂ (One flavor)

From this section, we start computations using the non-Abelian bosonization. The utility of the bosonized form is that we can compute several quantities in terms of quark number and color densities, emphasizing how differently a quark chemical potential acts on quark numbers and colors. Another utility is that we can write explicit relations between chiral and quark number densities which are useful to consider issues of the chiral symmetry breaking/restoration in quark matter.

3.1 Preliminaries

We review the non-Abelian bosonization rules, to the extent necessary for our arguments (For quick introduction, see [24]). The rules take compact forms by using lightcone coordinates $x_{\pm} = x^{\mp}/2 = x_0 \pm x_1$, and $\partial_{\pm} = 2\partial^{\mp} = \partial_0 \pm \partial_1$. The currents for $U(1)$ and $SU(N_c)$ chiral charges are

$$\begin{aligned} J_- &= i \frac{N_c}{4\pi} U \partial_- U^{\dagger} = : \psi_-^{\dagger} \psi_- :, \quad J_+ = i \frac{N_c}{4\pi} U^{\dagger} \partial_+ U = : \psi_+^{\dagger} \psi_+ :, \\ J_-^A &= \frac{i}{2\pi} \text{tr}[h \partial_- h^{\dagger} t_A] = : \psi_-^{\dagger} t_A \psi_- :, \quad J_+^A = \frac{i}{2\pi} \text{tr}[h^{\dagger} \partial_+ h t_A] = : \psi_+^{\dagger} t_A \psi_+ :, \end{aligned} \quad (8)$$

with fields $U(x)$ and $h(x)$ which are frequently written as $U(x) = e^{i\phi(x)}$ and $h(x) = e^{it_A \pi_A(x)}$. We have normal ordered currents and subtracted infinite constants. These currents are related to J_{μ} and $J_{\mu 5}$ as

$$J_{\mu} = \begin{pmatrix} J_0 \\ J_1 \end{pmatrix} = \begin{pmatrix} J_- + J_+ \\ J_+ - J_- \end{pmatrix}, \quad J_{\mu 5} = \epsilon_{\mu\nu} J^{\nu} = \begin{pmatrix} J_- - J_+ \\ J_- + J_+ \end{pmatrix}. \quad (9)$$

In chiral limit, they satisfy $\partial^{\mu} J_{\mu} = \partial^{\mu} J_{\mu 5} = \partial_{\pm} J_{\mp} = 0$. Similar relations hold for J^A . The operator responsible for the chiral density is

$$\bar{\psi}_+^a \psi_-^b = c(M) (h^{ab})_M (U)_M, \quad (10)$$

where a, b is color indices of fermions. Here $c(M)$ is a renormalization constant, and a subscript M means that operators are normal ordered at a scale M [35]. Note that the chiral density and the quark number density are characterized by common fields U and h , so once we know behaviors of these fields, we also know both densities simultaneously.

The kinetic part of the fermion becomes

$$\int d^2x \bar{\psi}(x) i \not{\partial} \psi(x) \longrightarrow S_{k=N_c}^{U(1)}[U] + S_{k=1}^{WZW}[h], \quad (11)$$

where $S_{k=N_c}^{U(1)}[U]$ is an action of free massless boson,

$$S_{k=N_c}^{U(1)}[U] = \frac{N_c}{8\pi} \int d^2x (\partial_\mu U^\dagger \partial^\mu U), \quad (12)$$

and $S_{k=1}^{WZW}[h]$ is Wess-Zumino-Novikov-Witten (WZNW) action [21],

$$S_k^{WZW}[l] = \frac{k}{8\pi} \text{tr} \left[\int d^2x \partial_\mu^\dagger l \partial^\mu l + \frac{2}{3} \int d^3x \epsilon^{\mu\nu\lambda} (l^\dagger \partial_\mu l) (l^\dagger \partial_\nu l) (l^\dagger \partial_\lambda l) \right], \quad (13)$$

with level $k = 1$, and $l = h$. While the β function of the non-linear σ model shows an asymptotic free behavior, the WZW term cancels out it. Thus the action is conformal at quantum level. The scale Λ_{QCD} will be introduced by confining current-current interactions ($g \sim \Lambda_{\text{QCD}}$).

Now we found one of the utilities of the non-Abelian bosonization. The colored currents include only colored boson fields $h(x)$, and do not depend on other densities in chiral limit: The actions for $U(1)$ quark number and color charge sectors decouple. Only the color sector includes the dimensionful quantity, i.e., the gauge coupling constant with dimension one. The decoupled $U(1)$ action is described by the free bosons and is conformal.

3.2 The infrared fluctuations and the spontaneous symmetry breaking

Before proceeding to our main discussions, first let us specify peculiarities in (1+1) dimensions. We will shortly take a glance at the relationship between the conformal property in the $U(1)$ action and Coleman-Mermin-Wagner theorem: the spontaneous symmetry breaking is forbidden in (1+1) dimensions [14].

Because of the separation of the $U(1)$ and color sectors, the chiral condensate can be written in the factorized form,

$$\langle \bar{\psi}_+ \psi_- \rangle = c(M) \langle \text{tr}[h]_M \rangle \langle U_M \rangle. \quad (14)$$

This matrix element vanishes due to the infrared divergence in the propagator of the massless $U(1)$ boson which characterize the phase degrees of freedom in the chiral space. Intuitively, this reflects that phase fields in the chiral space rotate rapidly, without taking any particular direction. An explicit expression

is $(\beta = (4\pi/N_c)^{1/2})$ [35]

$$\langle U_M \rangle = \langle (e^{i\beta\varphi(x;m_\varphi)})_M \rangle = e^{-\frac{\beta^2}{2}\Delta(M;m_\varphi)} = e^{\frac{\beta^2}{8\pi} \ln \frac{m_\varphi^2}{M^2}} = \left(\frac{m_\varphi}{M} \right)^{1/N_c}. \quad (15)$$

Witten first observed this sort of N_c dependence in (1+1) dimensional correlation functions of chiral operators, which behave as $\sim 1/|\vec{x} - \vec{y}|^{1/N_c}$ [13]. Here Δ is a propagator of the boson φ , and m_φ is the mass of φ which should be taken to be zero at the end of the calculations.

This expression is one example which illustrates subtleties in the limiting order, large N_c and chiral limit. If we start with the strict chiral limit, we must first take $m_\varphi \rightarrow 0$ limit before taking the large N_c limit. Thus the matrix element vanishes.

The exception is the case with finite volume or with the infrared momentum cutoff. This is a typical situation studied in seminal works. They essentially yield similar effects to the introduction of m_φ . Once we regularize these infrared fluctuations, we can simply take the large N_c limit,

$$\langle \bar{\psi}_+ \psi_- \rangle = c(M) \langle \text{tr}[h]_M \rangle \times \left(\frac{m_\varphi}{M} \right)^{1/N_c} \longrightarrow c(M) \langle \text{tr}[h]_M \rangle. \quad (16)$$

Here the m_φ dependence disappears as $N_c \rightarrow \infty$. The renormalization constant and the value of $\langle \text{tr}[h]_M \rangle$ will be fixed in the next subsection. In the following we will frequently omit a subscript M if it does not play an essential role.

Finally we would like to recall Witten's argument [13] that phase fields in (1+1) dimensions should not be identified as Goldstone bosons. While both of them share common features as phase fluctuations, they play quite different roles in the chiral limit. The former belongs to the ground state properties, while the latter appears as an excitation from the vacuum. This aspect becomes a little bit vague once we introduced an explicit breaking of the chiral symmetry, since phase fluctuations become physical excitation modes after the vacuum chose a particular direction in the chiral space. In what follows, we will not argue issues which are very sensitive to this conceptual issues. We will regard phase fluctuations as excitation modes.

3.3 A mass perturbation

Now let us introduce a current quark mass term

$$\mathcal{L}_m = -m_q(\bar{\psi}_+ \psi_- + \bar{\psi}_- \psi_+) = -m_q \times c(M)(\text{tr}[h]U + \text{tr}[h^\dagger]U^\dagger). \quad (17)$$

which explicitly breaks the conformal symmetry in the $U(1)$ sector. Besides the infrared regularization, the mass term couples the $U(1)$ and color sectors, thus it is no longer possible to investigate these sectors separately. Thus from now we rely on the large N_c limit. Then we can apply a probe approximation which significantly simplifies the arguments [8].

The point is that while the $U(1)$ sector provides $O(N_c)$ contributions at most, those from quantum fluctuations in the color sector is $O(N_c^2)$ because of $O(N_c^2)$ degrees of freedom. The confining interactions generate a mass gap for the colored particles, so we can replace $\text{tr}h$ with $\langle \text{tr}h \rangle$ in arguments of the low energy phenomena. The value of $\langle \text{tr}h \rangle$ is supposed to be well-approximated by that computed without a current quark mass which is expected to act as a small perturbation to the mass gap $\sim \Lambda_{\text{QCD}}$.

We analyze the $U(1)$ sector under such a background. Then the effective action for the low energy excitations is

$$S^{\text{eff}}[U] \simeq \frac{N_c}{8\pi} \int d^2x \left[(\partial_\mu U^\dagger \partial^\mu U) + m_\varphi^2 (U + U^\dagger - 2) \right], \quad (18)$$

where we have subtracted a constant to normalize the action. We have also used $\langle \text{tr}h \rangle = \langle \text{tr}h^\dagger \rangle$ and defined $m_\varphi^2 = -m_q \times 8\pi c(M) \langle \text{tr}[h] \rangle / N_c$ for later convenience. Of course we can arrive at the similar Lagrangian following usual steps, the bottom up construction with the chiral symmetry constraints. Only difference is that in the above treatment the role of the colored sector was explicit.

Now we take the expression $U = e^{i(4\pi/N_c)^{1/2}\varphi}$ to canonically normalize the kinetic term for quantum excitations. Then the action for φ becomes

$$\begin{aligned} S^{\text{eff}}[\varphi] &= \int d^2x \left(\frac{1}{2} (\partial_\mu \varphi)^2 + \frac{N_c m_\varphi^2}{4\pi} \left(\cos(\sqrt{4\pi/N_c} \varphi) - 1 \right) \right) \\ &= \int d^2x \frac{1}{2} \left((\partial_\mu \varphi)^2 - m_\varphi^2 \varphi^2 \right) + O(1/N_c). \end{aligned} \quad (19)$$

At large N_c , m_φ should coincide with the mass of the lowest mode of the Bethe-Salpeter equations, computed by 't Hooft. He computed the pole mass of the channel J_- in the lightcone gauge. In the bosonized form, the long range behavior of the corresponding correlator is $(x \gg (g^2 N_c)^{-1/2})$

$$\langle J_-(x) J_-^\dagger(0) \rangle \sim \langle \partial_- \varphi(x) \partial_- \varphi(0) \rangle, \quad (20)$$

so the pole should coincides with m_φ^2 . Matching 't Hooft's result with that in the bosonized form,

$$m_\varphi^2 = m_q \sqrt{\frac{4g^2 N_c \pi}{3}} = -m_q \frac{8\pi c(M) \langle \text{tr}[h] \rangle}{N_c}, \quad (21)$$

then we can fix the scale, $c(M)\langle\text{tr}[h]\rangle$. Using these constants, we can see the value of the chiral condensate. Since m_φ regulates infrared behaviors of φ , the $U(1)$ sector now has a nonvanishing expectation value. At large N_c , we have

$$\langle\bar{\psi}\psi\rangle = 2c(M)\langle\text{tr}[h]\rangle = -N_c\sqrt{\frac{g^2N_c}{12\pi}}. \quad (22)$$

This result was originally derived by Zhitnitsky using the current algebra plus the operator product expansion [9]. We reproduce this result simply because the bosonization procedures correctly implement the approximate chiral symmetry, thus satisfy the current algebra aspects. For later convenience, we write the pion mass in terms of the chiral condensate

$$m_\varphi^2 = -\frac{4\pi m_q}{N_c}\langle\bar{\psi}\psi\rangle. \quad (23)$$

4 One baryon, two baryons, and finite baryon density (One flavor)

From this section, we analyze the finite density problems using the non-Abelian bosonization. We will first discuss the one flavor case, and the two flavor extension will be discussed in Sec.5.

While our main concern in this paper is the properties of Quarkyonic matter, perhaps it is instructive to discuss the properties of baryonic matter in light of the present framework. Therefore we will start our discussions from a single baryon. Then we argue a baryon-baryon interaction, and finally move to the Quarkyonic matter.

The outline our discussions is the following: The ground state baryon is constructed as a soliton since we fully bosonize the fermion operators. The solitonic construction turns out to be less problematic in (1+1) dimensions than in (3+1) dimensions. Unfortunately, in spite of the presence of the confining force, the ground state baryon in QCD_2 tells us little about the N_c -quarks bound by the color fluxes. We will interpret this result in light of the charge-color separation, which is absent in (3+1) dimensions. So we can not discuss detailed structural changes of baryons in terms of fermionic contents or flux tubes, in a manner applicable to the (3+1) dimensional cases⁹. We also see

⁹ The fermionic description is found in Ref. [27]. The energy contains the IR divergent piece as a consequence of the confining models. Without confinement, the single fermion properties become well-defined due to the smallness of the residual interactions. An interested reader should consult with, for instance, papers [27,40] for the Gross-Neveu model, papers [36] for the NJL model for baryons, and a recent paper [37] for the nuclear-quark matter transition.

that a single baryon accompanies a single chiral spiral. After showing the operator relation special to (1+1) dimensions, we will give its qualitative picture which, to some extent, may be extended to the (3+1) dimensional considerations.

Next the baryon-baryon interaction is discussed. At large N_c , the strongest force originates from the $O(N_c)$ quark density, leading to the coherent meson exchange with the large amplitude¹⁰. The force is purely repulsive, and we did not find the attractive part which, in (3+1) dimensions, may emerge from the σ exchange¹¹. At higher density, this force from $U(1)$ charges will remain important, in sharp contrast to the forces from the non-Abelian charges like isospins which will eventually cancel out one another. Thus irrespective of contents of flavors, the relevance of the strong repulsive force grows as increasing density, eventually invalidating the baryon based descriptions. We will enter the regime where the quark picture is necessary to account for the bulk part of the Fermi sea.

Finally we argue the Quarkyonic matter regime. The basic degrees of freedom are a quark and a quark-hole which form the color singlet mesonic objects. The condensations of them provide the chiral spirals. In spite of the homogeneous distributions of chiral densities, quark number density is nearly uniform. We will also see the fundamental excitations are particles and holes, and there is no strong motivation to consider baryonic excitations. The n (n : positive integer) particle-hole picture provides much more general descriptions than a baryon and a baryon-hole excitation, or a baryonium bound state.

4.1 One baryon as a topological object

With a boundary condition for a topological charge, we can find a solution for coherent configurations $\bar{U} = e^{i\phi}$ regarding ϕ as $O(N_c^0)$ quantity. The action becomes the sine-Gordon model,

$$S^{\text{eff}}[\phi] = \frac{N_c}{8\pi} \int d^2x \left[(\partial_\mu \phi)^2 + 2m_\phi^2 (\cos \phi - 1) \right], \quad (24)$$

whose properties are well-investigated [7]. At large N_c , stationary phase approximation is applicable due to an overall N_c factor of the action. Using

¹⁰ All other meson exchanges happen only as quantum processes, so amplitudes are suppressed by $1/N_c$.

¹¹ If the σ meson entirely originates from the correlated 2π exchanges, it should be assigned as quantum processes in the present framework.

Bogomol'nyi's trick, we have the lower bound of the energy,

$$E^{\text{eff}}[\phi] = \frac{N_c}{8\pi} \int dz \left(\partial_z \phi \mp 2m_\varphi \sin \frac{\phi}{2} \right)^2 \pm \frac{N_c m_\varphi}{2\pi} \int_{\phi(-\infty)}^{\phi(+\infty)} d\phi \sin \frac{\phi}{2} \geq |N_B| \times \frac{2N_c m_\varphi}{\pi}, \quad (25)$$

where $\phi(\pm\infty)$ must be $2\pi \times$ integer. The equality holds only when the first bracket becomes zero. It is satisfied only by the topological charge one solution, whose configuration and energy are,

$$\phi(z; z_0) = 4 \tan^{-1} e^{-m_\varphi(z-z_0)}, \quad E = \frac{2N_c m_\varphi}{\pi}, \quad (26)$$

where z_0 is a free parameter to characterize a center of a single baryon. Here ϕ goes to 0 as $z \rightarrow \infty$ and to 2π as $z \rightarrow -\infty$, as shown in the left panel of Fig.6. The baryon density is localized around $z = z_0$ as (the right panel of Fig.6)

$$J_0 = -\frac{N_c}{2\pi} \partial_z \phi = \frac{N_c m_\varphi}{4\pi \cosh(m_\varphi(z-z_0))}, \quad (27)$$

By integrating J_0 with respect to z , we can see its quark number is N_c .

With expressions (26) and (27), the relationship between a quark number and chiral spirals is explicit. The scalar and pseudoscalar chiral densities are (here we attach a minus sign in front of $\Delta \equiv |\langle \bar{\psi}\psi \rangle_{\text{VAC}}|$ since $\langle \bar{\psi}\psi \rangle_{\text{VAC}} < 0$),

$$\langle \bar{\psi}\psi(z) \rangle_B = \langle \bar{\psi}_+\psi_- \rangle_B + \langle \bar{\psi}_-\psi_+ \rangle_B = -\Delta \cos \phi(z; z_0), \quad (28)$$

$$\langle \bar{\psi}i\gamma_5\psi(z) \rangle_B = -i(\langle \bar{\psi}_+\psi_- \rangle_B - \langle \bar{\psi}_-\psi_+ \rangle_B) = -\Delta \sin \phi(z; z_0), \quad (29)$$

so we find one chiral spiral around a single baryon. It is natural to expect more chiral spirals when we have a larger number of baryons, or more generically, quark number density. We will see this explicitly later.

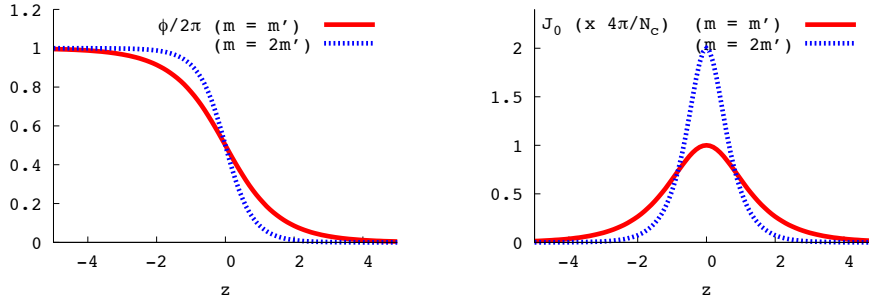


Fig. 6. The behaviors of ϕ field divided by 2π (left panel) and quark number current j_0 divided by $N_c/4\pi$ (right panel) as functions of z with some arbitrary dimensionful unit, m'^{-1} . We chose z_0 to be 0. For each plot, we took $m_\varphi = m'$ and $m_\varphi = 2m'$ to see the mass dependence.

For future references, perhaps it is useful to rephrase the emergence of chiral spirals in a different way, without emphasizing (1+1) dimensional operator relations. Note that $\langle \bar{\psi}_+ \psi_- \rangle$ ($\langle \bar{\psi}_- \psi_+ \rangle$) expresses an average density of pairs co-moving in the $-z$ ($+z$) direction. Baryons make different potentials for pairs moving in opposite directions. Accordingly there is a mismatch in densities $\langle \bar{\psi}_+ \psi_- \rangle$ and $\langle \bar{\psi}_- \psi_+ \rangle$ near the baryon, so that $\langle \bar{\psi} i \gamma_5 \psi \rangle$ does not vanish. We can repeat similar arguments in higher dimensions, once we replace γ_5 with $\gamma_0 \gamma_j$, whose eigenvalues characterize moving directions of particles in a similar way as γ_5 does in (1+1) dimensions [3,16].

Finally we would like to examine qualitative differences in solitonic constructions of baryons in (1+1) and (3+1) dimensions. In the former, computations can be closed within dynamics around the scale, $m_\varphi \ll \Lambda_{\text{QCD}}$. This is in sharp contrast to (3+1) dimensional cases [38]: To get stable soliton solutions in the chiral Lagrangian, we need to equate the leading order with the next leading order of the derivative expansions, $(\sim \partial/\Lambda_{\text{QCD}})^n$. But once the LO and NLO become comparable, then, in principle, all possible higher orders become relevant [39]. The effects of higher orders are needed to be computed or be replaced with quark degrees of freedom.

Another important difference is that the former can be constructed from $U(1)$ bosons only, instead of flavored pions in (3+1) dimensional solitons. It is natural to have the coherent configurations, $O(N_c)$ amplitude of $U(1)$ bosons, since quark number density is $O(N_c)$ inside of the baryon.

Taking into account these differences between (1+1) and (3+1) dimensions, the former case has less problems to apply the solitonic picture to the ground state baryon. Presumably this simplicity comes from the fact that we see remnants of the charge-color separation. Such a separation is broken only via a term proportional to a small current quark mass, and the dynamics of colors only plays a very indirect role. Thus we expect that baryons discussed here have little to do with the picture of N_c -quarks bound by the color fluxes. This means that our approach can not answer to several interesting questions such

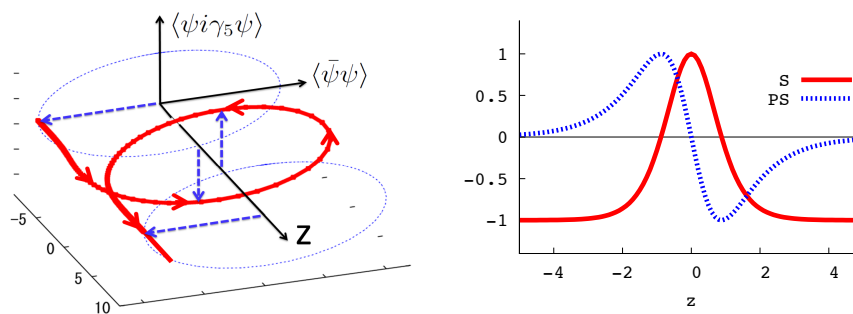


Fig. 7. The behaviors of scalar (S) $\langle \bar{\psi} \psi \rangle$ and pseudo scalar (PS) $\langle \bar{\psi} i \gamma_5 \psi \rangle$ chiral condensates as functions of z . The unit of condensates is Δ . Left panel: 3D plot of the chiral spiral. Right panel: Separate plots of condensates.

as how quark wavefunctions or color flux tubes inside of baryons change as increasing density.

4.2 Two baryons and interactions

As we already saw in the one baryon sector, Bogomol'nyi's bound is satisfied only by a single baryon solution. It means that the energy of two baryons is always larger than twice of single baryon energy,

$$E_{B=2} > 2E_{B=1} . \quad (30)$$

The additional energetic cost comes from the repulsive interaction between two baryons. Its asymptotic form is (R is the distance between two baryons)

$$V(R) \sim N_c m_\varphi e^{-m_\varphi R} . \quad (31)$$

When $R \sim m_\varphi^{-1}$, the strength of repulsion becomes the same order as the single baryon mass.

How generic is this sort of the strong repulsive force in general dimensions? In QCD₄, we know that the ω meson exchanges in nuclear forces are strong and repulsive. One interpretation of the strength is that it comes from the quark number of $O(N_c)$ which produces a large number of $U(1)$ mesons of $O(N_c)$. The repulsive feature presumably comes from an additive property of $U(1)$ charges, in sharp contrast to other non-Abelian charges such as isospins which stays at $O(N_c^0)$ for the ground state baryons.

We expect that this viewpoint be increasingly important at higher quark density. While non-Abelian charge densities such as colors or isospins cancel one another and remain at $O(1)$, the enhancement of the quark number density is not tempered at large density. Then strong repulsive interactions become increasingly important, and then completely change baryon structures. Eventually computations based on the quasi-particle picture of baryons break down, implying that the quarks become reasonable effective degrees of freedom to describe most part of the Fermi sea.

4.3 Finite density (one flavor)

Since two baryon interactions are repulsive, baryonic matter starts to appear from the critical quark chemical potential, $\mu_c \equiv M_B/N_c = 2m_\varphi/\pi \sim 0.7m_\varphi$. In the following, the canonical approach is used. Since we have a large number of quarks, the leading contributions can be computed by studying coherent

field configurations. With the coherent field expression $U \sim e^{i\phi}$, a total quark number of the system per period L is

$$N_q = - \int_0^L dz J_0[\phi] = - \frac{N_c}{2\pi} \int_0^L dz \partial_z \phi = - \frac{N_c}{2\pi} [\phi(L) - \phi(0)] = N_c N_B. \quad (32)$$

Below we take $\phi(L) - \phi(0) = -2\pi N_B$ so that $n_B = N_B/L$ represents a baryon density¹². We will use $p_f = \pi n_B$ in the following.

With this constraint of a finite quark number, we first determine a static background in the large N_c stationary phase approximation. The Hamiltonian for static coherent fields is¹³

$$\begin{aligned} \frac{E[\phi]}{L} &= \frac{N_c}{4\pi L} \int dz \left(\frac{1}{2} (\partial_z \phi)^2 - m_\varphi^2 (\cos \phi - 1) \right) \\ &= \frac{N_c}{2\pi} (2m_\varphi^2 + p_f^2) + \frac{N_c}{8\pi L} \int dz \left\{ (\partial_z \tilde{\phi})^2 - 2m_\varphi^2 \cos(\tilde{\phi} - 2p_f z) \right\}, \end{aligned} \quad (33)$$

where we have decomposed $\phi(z)$ field into $\phi_0(z) \equiv -2p_f z$ and $\tilde{\phi}(z)$. So $\tilde{\phi}$ satisfies a periodic boundary condition, $\tilde{\phi}(0) = \tilde{\phi}(L)$, forming the manifold S_1 . To find a solution for coherent configurations, we have to solve the following equation,

$$\partial_z^2 \tilde{\phi} - m_\varphi^2 \sin(\tilde{\phi} - 2p_f z) = 0. \quad (34)$$

The equation has been investigated extensively. It is known that solitonic configurations are general solutions which interpolate well-separated baryonic soliton configurations at low density and uniform quark number distributions at high density (For intensive discussions, see [40]).

We will not repeat detailed analyses here but just quote some results about high density to assure our qualitative discussions in Sec.2.

In chiral limit, $\tilde{\phi}(z) = 0$ is the solution which means that the baryon density is uniform. The colored sector and the Lagrangian for quantum fluctuations are exactly the same as the vacuum. The chiral condensate behaves as $\langle \bar{\psi}_\mp \psi_\pm \rangle = \Delta e^{\pm i\phi} = \Delta e^{\pm 2ip_f z}$, and form the chiral spirals. The coefficient Δ equals to the

¹² We require quantum fluctuations φ to be normalizable modes, so that the expression (32) saturates the average baryon density.

¹³ We assume that $\tilde{\phi}$ does not contain any constant, since it can be always absorbed by shifting $2p_f z \rightarrow 2p_f(z - z_0)$.

vacuum value¹⁴. The classical energy density is

$$\frac{E[\tilde{\phi} = 0]}{L} = \frac{N_c}{2\pi} p_f^2. \quad (35)$$

The density contributions to the energy density is just those of free fermions.

Next let us consider the case of massive fermions in asymptotically high density. If we rewrite Eq.(34) by scaling a variable as $z' = 2p_f z$,

$$\partial_z^2 \tilde{\phi} + \left(\frac{m_\varphi}{2p_f} \right)^2 \sin(z' - \tilde{\phi}) = 0, \quad (36)$$

so $\tilde{\phi} \sim (m_\varphi/p_f)^2$, and we can organize expansions. An asymptotic behavior,

$$\tilde{\phi}^{(1)} \simeq \left(\frac{m_\varphi}{2p_f} \right)^2 \sin(2p_f z), \quad (37)$$

satisfies Eq.(34) up to $O(m_\varphi^2/p_f^2)$. This expression illustrates that roles of mass become less relevant as density increases.

With the expression (37), we can compute a number of quantities of interest (Summary of distributions can be found in Fig.8.). The oscillation of the chiral condensate is slightly deformed as

$$\langle \bar{\psi} \psi \rangle \simeq \Delta \cos(\phi_0 + \tilde{\phi}^{(1)}) = \Delta \cos \left(2p_f z - \frac{m^2}{4p_f^2} \sin(2p_f z) \right), \quad (38)$$

and $\langle \bar{\psi} i\gamma_5 \psi \rangle$ also oscillates in the similar way. The baryon density also acquires modulations,

$$\langle J_0 \rangle \simeq -\frac{N_c}{2\pi} \partial_z [\phi_0 + \tilde{\phi}^{(1)}] = \frac{N_c}{2\pi} \times 2p_f \left\{ 1 - \frac{m_\varphi^2}{4p_f^2} \cos(2p_f z) \right\}. \quad (39)$$

In average, this solution does not contribute to the total baryon charge, since it just fluctuates around zero. At high density, prominent structures in quark number density is eventually buried in the average quark number background. The average energy density for $\tilde{\phi} = \tilde{\phi}^{(1)}$ is

$$\frac{E[\tilde{\phi}^{(1)}]}{L} = \frac{N_c p_f^2}{2\pi} \left\{ 1 + 2 \left(\frac{m_\varphi}{p_f} \right)^2 - \frac{1}{32} \left(\frac{m_\varphi}{p_f} \right)^4 + O(m_\varphi^6/p_f^6) \right\}, \quad (40)$$

¹⁴ It might seem strange that we get chiral spirals without any energetic minimization with respect to the chiral condensate. Actually, the modulus of chiral condensates is served from the color sector, independently from properties of the $U(1)$ sector. If one hopes to see energetic differences with or without chiral condensates, one must derive an expression of the energy in the color sector.

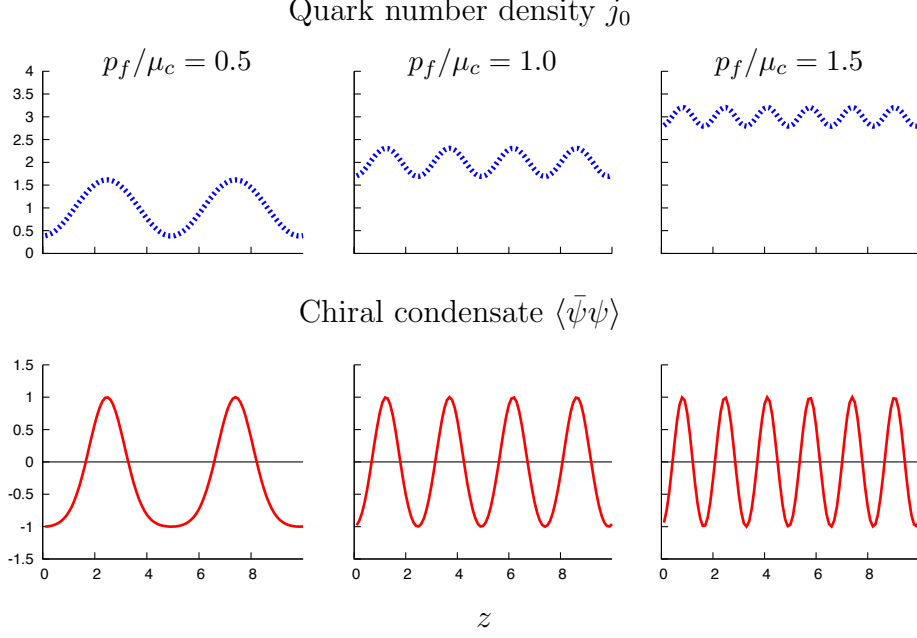


Fig. 8. The behaviors of quark number density (upper panels) and chiral scalar density (low panels) as functions of z with different quark densities $p_f/\mu_c = 0.5, 1.0, 1.5$. (The units of z , j_0 , $\langle\bar{q}q\rangle$ are m_φ^{-1} , $N_c\mu_c/2\pi$, Δ , respectively.)

where the second term comes from the vacuum constant, while the third term expresses corrections from the density wave modulations.

An easy way to interpret expressions (38), (39), and (40), in the fermionic language is to employ a particle-hole picture in the quark Fermi sea (Fig.9). When baryons largely overlap, quark number distribution is almost uniform. Deviations from such distributions can be regarded as corrections caused by particle-hole degrees of freedom. Indeed, spatial modulations have a period $1/2p_f$, reflecting that condensations are driven by co-moving particle-hole pairs near the Fermi surface. Note also that the shape of each peak in the baryon density (39) is very different from that of the single baryon solution.

Based on the above arguments, it seems better to regard baryonic configurations just as quark number localizations and defects, made of n particle-hole pairs, where n is a positive integer. They contains a wider class of excitations than baryon and baryon-hole excitations, because n need not to be quantized to a particular number, N_c . Therefore we have no strong motivation to focus on baryon excitations in usual sense, in which the color-singletness is maintained within a single baryon or a single baryon-hole, by definition.

One might think a possibility of a baryon and a baryon-hole bound state and its condensation. But it should be described not only by the N_c particle-hole pairs, but also by $N_c - 1$, $N_c - 2$, ... particle-hole pairs because of the partial annihilations of particle-holes. Again we have no good reason to start with

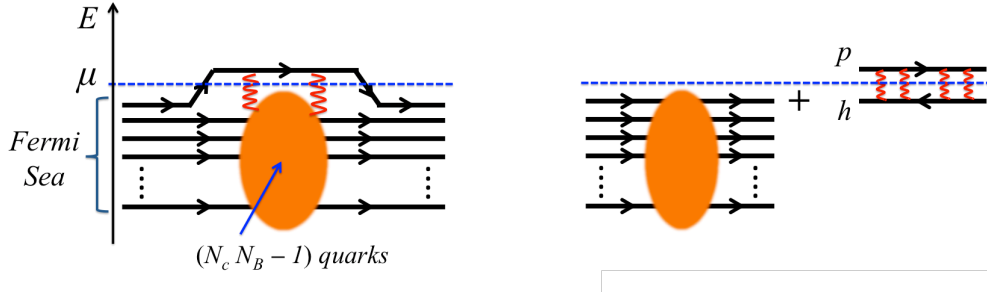


Fig. 9. A schematic picture for a particle-hole excitation. The case with total baryon number, N_B , is illustrated. (Left) The interactions between one quark excitation and $(N_c N_B - 1)$ quarks. (Right) The equivalent diagram in the particle-hole picture.

baryons and baryon-holes for the considerations of the condensation phenomena.

A more nontrivial possibility is the dibaryon type condensation such as baryon superfluidity. But in QCD_2 with one flavor, we observed only the repulsive force at large N_c , so such phenomena can occur only after the subleading effects of $1/N_c$ are included. To explore this possibility for finite N_c , we need quantitative arguments. We leave it for future studies.

With combining all these pictures together, at least in the large N_c limit, our system is naturally viewed as a system with the Fermi sea of weakly coupled quarks plus mesonic excitations of particle-hole type. These arguments are consistent with discussions in Sec.2 which are based on the fermionic language.

5 Two flavors

In this section, we extend analyses to two flavor cases with u and d quarks, keeping the vector symmetry $SU(2)_V$ by taking equal current quark masses $m_q = m_u = m_d$. While most of treatments are the same as before, it is interesting to see the possibility of the chiral spirals including the flavor rotations such as $\langle \bar{\psi} i \gamma_5 \tau_3 \psi \rangle$. This issue may have phenomenological relevance to stars via the spontaneous generation of magnetic fields of the QCD scale.

According to Vafa-Witten theorem [41] at zero density, the vector-like theories with current quark masses can not have the flavor symmetry breaking. However, several conditions used in that proof can not be applied in the presence of the chemical potential, so this problem is interesting in its own right. In the following, we will not turn on electromagnetic interactions, but just see what happens in the QCD sector. (In case of NJL₂ studies in the presence of isospin chemical potential, see Ref. [42].)

We will see that, in the present model, the chiral spirals mainly occur between $\langle \bar{\psi}\psi \rangle$ and $\langle \bar{\psi}i\gamma_5\psi \rangle$. The rotations including $\langle \bar{\psi}i\gamma_5\tau_a\psi \rangle$ can also occur, but it is order of m_φ^2/μ^2 compared to $U(1)$ channel, so will eventually disappear at high density. This can be interpreted as cancellations of non-Abelian charges at high density.

5.1 Vacuum

When we consider the multi-flavors, we have only to add slight modifications to previous treatments. The coefficients of $U(1)$ and color currents change as,

$$J_-(x) = i\frac{N_c N_f}{4\pi} U \partial_- U^\dagger, \quad J_-^A(x) = i\frac{N_f}{2\pi} \text{tr}[h \partial_- h^\dagger t_A], \quad (41)$$

and flavor currents are defined as

$$J_-^f(x) = i\frac{N_c}{2\pi} \text{tr}\left[g \partial_- g^\dagger \frac{\tau_f}{2}\right], \quad J_+^f(x) = i\frac{N_c}{2\pi} \text{tr}\left[g^\dagger \partial_+ g \frac{\tau_f}{2}\right], \quad (42)$$

where the g is a matrix field and τ_f is a flavor matrix. with normalization $\text{tr}[\tau_f \tau_{f'}] = 2\delta_{ff'}$. The operators for the chiral density are

$$\bar{\psi}_+^{ai} \psi_-^{bj} = c(M) (h^{ab})_M (U)_M (g^{ij})_M, \quad (43)$$

where i, j, \dots are flavor indices for the fundamental representation. The action for the fermion kinetic term is

$$\int d^2x \bar{\psi}(x) i \not{\partial} \psi(x) \longrightarrow S_{k=N_c N_f}^{U(1)}[U] + S_{k=N_c}^{\text{WZW}}[g] + S_{k=N_f}^{\text{WZW}}[h]. \quad (44)$$

The treatments of the colored interactions are the same as before, and in chiral limit, there is the charge-flavor-color separation.

Below we will consider $N_f = 2$, massive quarks. With current quark masses, we have the following terms after applying a probe approximation and using $\text{tr}[g] = \text{tr}[g^\dagger]$,

$$\begin{aligned} \mathcal{L}_m &= -m_q(\bar{\psi}_+\psi_- + \bar{\psi}_-\psi_+) \\ &\rightarrow \frac{N_c m_\varphi^2}{8\pi} \text{tr}[g](U + U^\dagger) = \frac{N_c N_f m_\varphi^2}{4\pi} \cos \Pi \cos \phi, \end{aligned} \quad (45)$$

where we parameterized $U = e^{i\phi}$, and for the matrix field,

$$g = e^{i\Pi_f \tau_f} = \cos \Pi + i \hat{\Pi}_f \tau_f \sin \Pi \quad (\Pi^2 = \Pi_f^2, \quad \hat{\Pi}_f = \Pi_f / \Pi). \quad (46)$$

This simple expression holds for $N_f = 2$, since $\{\tau_f, \tau_{f'}\} = 2\delta_{ff'}$.

From the form of Eq.(45), we can see that the trivial vacuum is found by choosing $(\phi, \Pi) = (0, 0)$ and (π, π) (modulo 2π), which maximizes the absolute value of the chiral condensate. On the other hand, the flavor or parity violating chiral condensates are

$$\bar{\psi} i\gamma^5 \psi \sim \text{tr}[g] (e^{i\phi} - e^{-i\phi}) \sim \cos \Pi \sin \phi, \quad (47)$$

$$\bar{\psi} \tau_f \psi \sim (\text{tr}[g\tau_f] e^{i\phi} + \text{tr}[g^\dagger \tau_f] e^{-i\phi}) \sim \hat{\Pi}_f \sin \Pi \sin \phi, \quad (48)$$

$$\bar{\psi} i\gamma^5 \tau_f \psi \sim (\text{tr}[g\tau_f] e^{i\phi} - \text{tr}[g^\dagger \tau_f] e^{-i\phi}) \sim \hat{\Pi}_f \sin \Pi \cos \phi, \quad (49)$$

becomes zero. The above expressions indicate that these condensates compete with the usual chiral condensate. The usual chiral condensate wins because of the mass term.

The action for quantum excitations can be obtained by expanding fields around this vacuum. Taking $U = e^{i(4\pi/N_c N_f)^{1/2} \varphi}$ and $g = e^{i(2\pi/N_c)^{1/2} \pi_f \tau_f}$, we have

$$S^{\text{eff}}[\varphi, \pi_f] = \int d^2x \frac{1}{2} \left((\partial_\mu \varphi)^2 + (\partial_\mu \pi_f)^2 - m_\varphi^2 (\varphi^2 + \pi_f^2) \right) + O(1/N_c^{1/2}). \quad (50)$$

The masses of bosons in $U(1)$ and $SU(2)$ are degenerate as a consequence of large N_c . At finite N_c , there are higher order interaction terms in $SU(2)$ sector, and they destroys such a degeneracy.

5.2 Finite density

Calculations of finite density case can be done as before. We again consider the canonical approach, and take the average isospin density zero. Then we have a periodic boundary condition, $\Pi_f(0) = \Pi_f(L)$. The static energy functional for coherent field configurations is

$$E[\tilde{\phi}, \Pi_f] = N_c N_f \frac{\pi N_B^2}{2L} + E_{kin} + E_m, \quad (51)$$

where (below we will explicitly substitute $N_f = 2$)

$$E_{kin}[\tilde{\phi}, \Pi_f] = \frac{N_c N_f}{8\pi} \int dz \left\{ (\partial_z \tilde{\phi})^2 + (\partial_z \Pi)^2 + (\partial_z \hat{\Pi}_f)^2 \sin^2 \Pi \right\}. \quad (52)$$

In chiral limit, it is clear that E_{kin} can be minimized by simply taking $\tilde{\phi} = \Pi = 0$. Thus $\phi = 2p_f z$, so chiral spirals appear only in the $U(1)$ sector. This reflects that an external source (a quark number constraint) is put only in the $U(1)$ sector.

Now let us see what happens if we include mass terms without explicitly breaking $SU(2)_V$. The energy density from the mass term is

$$\begin{aligned} E_m[\tilde{\phi}, \Pi_f] &= \frac{N_c N_f m_\varphi^2}{8\pi} \int dz \cos(2p_f z + \tilde{\phi}) \cos \Pi \\ &= \frac{N_c N_f m_\varphi^2}{16\pi} \int dz \left(\cos(2p_f z + \tilde{\phi} + \Pi) + \cos(2p_f z + \tilde{\phi} - \Pi) \right). \end{aligned} \quad (53)$$

We will assume that $\tilde{\phi}$ and Π do not contain any constant since they can be absorbed by shifting coordinate z . And it is more enlightening to rewrite kinetic terms,

$$E_{kin}[\tilde{\phi}, \Pi_f] = \frac{N_c N_f}{16\pi} \int dz \left\{ \left(\partial_z(\tilde{\phi} + \Pi) \right)^2 + \left(\partial_z(\tilde{\phi} - \Pi) \right)^2 + (\partial_z \hat{\Pi}_f)^2 \sin^2 \Pi \right\}. \quad (54)$$

From this form, $\partial_z \hat{\Pi}_f = 0$ reduces the energy, so we choose $\Pi = \Pi_3$ everywhere. Then we have two decoupled sine-Gordon models with finite density, whose variables are $\tilde{\phi} \pm \Pi_3$. We have only to borrow results of 1-flavor sine-Gordon model at finite density.

As in 1-flavor case, amplitudes of $\tilde{\phi}$ and Π_3 are $\sim m_\varphi^2/\mu^2$ at high density. From expressions in Eqs.(45) and (47)-(49), we found the following asymptotic behavior of condensates,

$$\langle \bar{\psi}\psi \rangle, \langle \bar{\psi} i\gamma^5 \psi \rangle \propto \Delta \cos \Pi \sim \Delta \times (1 + O(m_\varphi/\mu)^2), \quad (55)$$

$$\langle \bar{\psi} \tau_f \psi \rangle, \langle \bar{\psi} i\gamma^5 \tau_f \psi \rangle \propto \Delta \sin \Pi \sim \Delta \times O(m_\varphi/\mu)^2, \quad (56)$$

so the chiral spirals mainly occur in the $U(1)$ sector, while spirals with flavor breakings eventually disappear at high density. On the other hand, in relatively low density, we have solitonic lattices with mixture of a quark number and isospins.

6 Terms disturbing chiral spirals

In the preceding sections, we saw that the chiral symmetry is broken by chiral spirals when we have mechanisms to keep its modulus nonzero. We also observed that an explicit chiral symmetry breaking, i.e., a mass term, disturbs the chiral spirals, and such effects eventually disappear at high density. The purpose of this section is to generalize the above observation in such a way that we can classify several chiral effective models.

First let us rephrase the role of a mass in QCD₂ in the fermionic language,

$$-m_q \int dz (\bar{\psi}_- \psi_+ + \bar{\psi}_+ \psi_-). \quad (57)$$

Since we have the Fermi sea, it is more natural to measure momenta and energies from the Fermi surface. Replacing $\psi_{\pm} = \psi'_{\pm} e^{\pm i\mu z}$, we have

$$-m_q \int dz (\bar{\psi}'_- \psi'_+ e^{2i\mu z} + \bar{\psi}'_+ \psi'_- e^{-2i\mu z}). \quad (58)$$

Suppose that the ground state gives $\langle \bar{\psi}'_{\mp} \psi'_{\pm} \rangle \simeq \text{const.}$ This corresponds to chiral spiral solutions or uniform baryon distributions. For such a state, oscillating factors $e^{\pm 2i\mu z}$ wash out energetic contributions from Eq.(58). This is what we actually observed in Eqs.(39) and (40). If m_q is comparable to μ , the above state is not the ground state and we should search solitonic configurations. Thus the mass term disturbs the formation of the chiral spirals.

These arguments are useful to interpret results of other chiral models. For instance, 4-Fermi interaction terms in the chiral Gross-Neveu model (NJL₂) with the continuous chiral symmetry are

$$H_{int} = G \int dz \left((\bar{\psi}\psi)^2 + (\bar{\psi} i\gamma_5 \psi)^2 \right) = 4G \int dz \left((\bar{\psi}_+ \psi_-)(\bar{\psi}_- \psi_+) \right). \quad (59)$$

This form is unchanged when we rewrite fermion fields as $\psi_{\pm} = \psi'_{\pm} e^{\pm i\mu z}$ since oscillating factors cancel. Therefore the model at finite density takes the same form as that in vacuum, except the constant energy shift associated with changes of the fermion fields. The chiral spirals or uniform quark number distributions start to appear for an infinitesimal chemical potential – there is no phase transition with increasing density.

On the other hand, the discrete Gross-Neveu model takes the following interaction term,

$$\begin{aligned} H_{int} &= G \int dz (\bar{\psi}\psi)^2 \\ &= G \int dz \left(2(\bar{\psi}_+ \psi_-)(\bar{\psi}_- \psi_+) + (\bar{\psi}_+ \psi_-)^2 + (\bar{\psi}_- \psi_+)^2 \right) \\ &= G \int dz \left(2(\bar{\psi}'_+ \psi'_-)(\bar{\psi}'_- \psi'_+) + (\bar{\psi}'_+ \psi'_-)^2 e^{-4i\mu z} + (\bar{\psi}'_- \psi'_+)^2 e^{4i\mu z} \right). \end{aligned} \quad (60)$$

The second and third terms have oscillating factors, and disturb the formation of the chiral spirals. Thus chiral spirals and baryons can appear only after μ exceeds some critical value – there is a phase transition in contrast to the continuous model. At larger density, oscillating terms become less relevant, and the discrete model approaches to the continuous one. Thus at high density, this model can be regarded as NJL₂.

These aspects are sometimes not manifest in the mean field energy functionals. Let us consider the discrete Gross-Neveu model. Typically one takes ansatz such as $\langle \bar{\psi}\psi \rangle \sim 2\Delta \cos(qz) \equiv S$. This can be interpreted as

$$(\bar{\psi}\psi)^2 = \left((\bar{\psi}_- \psi_+ - \Delta e^{iqz}) + (\bar{\psi}_+ \psi_- - \Delta e^{-iqz}) + S \right)^2. \quad (61)$$

But the confusing point is that the final expression of the mean-field energy functional is characterized by $\langle \bar{\psi}\psi \rangle$ only, and roles of $\langle \bar{\psi} i\gamma^5 \psi \rangle$ condensate and chiral spiral structures are hidden. To see it, we have to explicitly calculate the condensate, or to construct the effective potential by inserting an infinitesimal external field.

Finally let us apply these arguments to the chiral spirals or crystal structures in higher dimensional systems. Consider states near the region ($p_z \sim \pm\mu$, $\vec{p}_T \sim 0_T$). By redefining fields $\Psi \rightarrow e^{i\mu z \gamma^0 \gamma^z} \Psi = e^{\pm i\mu z} \Psi_{\pm}$ (Ψ is a fermion field in higher dimensions), the fermionic kinetic term with a chemical potential becomes

$$\mathcal{L}^{kin} = \bar{\Psi}_+ i\partial_- \Psi_+ + \bar{\Psi}_- i\partial_+ \Psi_- + \bar{\Psi}_+ i\partial_T \Psi_- e^{-2i\mu z} + \bar{\Psi}_- i\partial_T \Psi_+ e^{2i\mu z}, \quad (62)$$

so transverse kinetic terms disturb the chiral spiral rotations between $\langle \bar{\Psi}\Psi \rangle$ and $\langle \bar{\Psi} \gamma^0 \gamma^z \Psi \rangle$. This field redefinition is useful as far as we consider only modes with $p_T \ll 2\mu$. It means that chiral spiral condensations along z direction can be made of particle-hole in the limited domain of p_T .

Besides the aforementioned roles, transverse kinetic terms include coupling between Ψ_+ and Ψ_- fields, and break the charge-color separation. This is consistent with the fact that in dimensions larger than one, increase of quark density affects the color sector through screening effects.

7 Summary

In this paper, we have utilized QCD₂ to illustrate some concepts of Quarkyonic matter. While Quarkyonic matter should differ from conventional quark matter in the excitation modes, it should be distinguished from nuclear matter by bulk quantities. These aspects can be seen in quark matter in QCD₂, as a consequence that quark chemical potential acts very differently on quark number density and color density.

The nonperturbative dynamics near the Fermi surface play deterministic roles to classify the phase structure, since bulk contributions computed by weak coupling methods are approximately common for different phases. Whether excitations are deconfined quarks and gluons, or confined hadrons and glueballs, is a key issue to understand dynamical phenomena in cold quark matter.

Another relevant topic discussed in this paper was the inhomogeneous distributions of the chiral condensates and quark number densities. In our opinion, such inhomogeneous descriptions have potential relevance since they might smoothly interpolate the Fermi surface of Quarkyonic matter and very dense nuclear matter¹⁵. In both phases, excitations are confined, and chiral symmetry is broken.

Several other important effects have not been addressed. In particular, we have not discussed the color superconductivity [43] for which a number of colors are important. Since the formation of colored diquark condensates competes with the presence of confining forces, they must be taken into account simultaneously for more realistic considerations than those given in this paper.

Acknowledgments

The author would like to give special thanks to Y. Hidaka, L. McLerran, R.D. Pisarski, and A.M. Tsvelik during the collaborations related to this work. He also acknowledges G. Basar, D. Blaschke, M. Buballa, A. Cherman, T. Cohen, G.V. Dunne, E.J. Ferrer, K. Fukushima, L.Y. Glozman, K. Hashimoto, T. Hatsuda, V. Incera, T. Izubuchi, D.B. Kaplan, H.K. Lee, S. Nakamura, J.M. Pawłowski, M. Rho, B.J. Schaefer, S.-J. Shin, E. Shuryak, D.T. Son, and I. Zahed for enlightening discussions and/or critical comments which have forced the author to reconsider many basic concepts of Quarkyonic matter. This research is supported under DOE Contract No. DE-AC02-98CH10886 and Postdoctoral Research Program of RIKEN.

References

- [1] L. McLerran and R. D. Pisarski, Nucl. Phys. A 796 (2007) 83.

¹⁵To avoid confusions, we have to emphasize that this crystalization is very different from that occurred in the Skyrme crystals [44,45] or its holographic QCD version [46]. The latter appears at very low density, because of long range attractive potential of $O(N_c)$ much larger than kinetic energy of $P^2/2M_N \sim 1/N_c$ (Ref. [47] conjectured that this problem arises from the overestimated nucleon axial charge g_A in the N_c counting). This description contradicts with the real nuclear matter at low density, which are liquid-like rather than solid-like. In contrast, here we are discussing high density where repulsive hard cores of nucleons of $O(N_c)$ start to overlap, and nucleons can not move easily. This is the region where the nucleon Fermi sea starts to transform to the quark Fermi sea. The understanding of this region remains a difficult problem.

- [2] L. McLerran, K. Redlich and C. Sasaki, Nucl. Phys. A **824**, 86 (2009) [arXiv:0812.3585 [hep-ph]]; A. Andronic *et al.*, Nucl. Phys. B 837 (2010) 65; Y. Hidaka, L. D. McLerran and R. D. Pisarski, Nucl. Phys. B 808 (2008) 117; T. Brauner, K. Fukushima and Y. Hidaka, Phys. Rev. D 80 (2009) 074035 [Erratum-*ibid.* D **81**, 119904 (2010)]; K. Miura, T. Z. Nakano and A. Ohnishi, Prog. Theor. Phys. 122 (2009) 1045; S. Hands, S. Kim and J. I. Skullerud, Phys. Rev. D 81 (2010) 091502;
- [3] T. Kojo, Y. Hidaka, L. McLerran and R. D. Pisarski, Nucl. Phys. A **843**, 37 (2010) [arXiv:0912.3800 [hep-ph]].
- [4] T. Kojo, R. D. Pisarski and A. M. Tsvelik, Phys. Rev. D **82**, 074015 (2010) [arXiv:1007.0248 [hep-ph]].
- [5] G. 't Hooft, Nucl. Phys. B 75 (1974) 461.
- [6] C. G. Callan, N. Coote and D. J. Gross, Phys. Rev. D 13 (1976) 1649; I. Bars and M. B. Green, Phys. Rev. D 17 (1978) 537.
- [7] S. Coleman, *Aspects of Symmetry*, Cambridge University Press.
- [8] I. Affleck, Nucl. Phys. B 265 (1986) 448.
- [9] A. R. Zhitnitsky, Phys. Lett. B 165 (1985) 405 ; *ibid.* Phys. Rev. D 53 (1996) 5821
- [10] L. L. Salcedo, S. Levit and J. W. Negele, Nucl. Phys. B 361 (1991) 585; V. Schon and M. Thies, Phys. Lett. B 481 (2000) 299; L. D. McLerran and A. Sen, Phys. Rev. D 32 (1985) 2794; P. J. Steinhardt, Nucl. Phys. B 176 (1980) 100.
- [11] A. Armoni, Y. Frishman, J. Sonnenschein and U. Trittman, Nucl. Phys. B **537**, 503 (1999) [arXiv:hep-th/9805155].
- [12] V.L. Berezinski, Sov. Phys. JETP. 32 (1970) 493; J.M. Kosterlitz and D.J. Thouless, J. Phys. C 6 (1973) 1181;
- [13] E. Witten, Nucl. Phys. B 145 (1978) 110.
- [14] S. R. Coleman, Commun. Math. Phys. **31**, 259 (1973).
- [15] D.V. Deryagin, D.Y. Grigoriev, and V.A. Rubakov, Intl. Jour. Mod. Phys. A 7 (1992) 659.
- [16] E. Shuster and D.T. Son, Nucl. Phys. B 573 (2000) 434; B. Y. Park, M. Rho, A. Wirzba and I. Zahed, Phys. Rev. D 62 (2000) 034015.
- [17] D. Nickel, Phys. Rev. Lett. 103 (2009) 072301; *ibid.* Phys. Rev. D 80 (2009) 074025; S. Carignano, D. Nickel and M. Buballa, Phys. Rev. D 82 (2010) 054009.
- [18] R. Rapp, E. V. Shuryak and I. Zahed, Phys. Rev. D 63 (2001) 034008.
- [19] E. Nakano and T. Tatsumi, Phys. Rev. D 71 (2005) 114006; S. Maedan, Prog. Theor. Phys. 123 (2010) 285; M. Sadzikowski and W. Broniowski, Phys. Lett. B 488 (2000) 63; M. Sadzikowski, Phys. Lett. B 642 (2006) 238; T. L. Partyka

- and M. Sadzikowski, Jour. Phys. G **36** (2009) 025004; T. L. Partyka and M. Sadzikowski, *ibid.* arXiv:1011.0921 [hep-ph]. B. Bringoltz, JHEP **0703**, 016 (2007); I. E. Frolov, V. C. Zhukovsky and K. G. Klimenko, Phys. Rev. D **82** (2010) 076002.
- [20] S. Mandelstam, Phys. Rev. D **11**, 3026 (1975).
- [21] S. P. Novikov, Usp. Mat. Nauk **37N5**, 3 (1982); E. Witten, Commun. Math. Phys. **92**, 455 (1984).
- [22] P. Francesco, P. Mathieu, and D. Senechal, *Conformal Field Theory*, Springer.
- [23] A.M. Tsvelik, *Quantum Field Theory in Condensed Matter Physics*, Cambridge University Press.
- [24] I. Affleck, Nucl. Phys. B **265** (1986) 409.
- [25] Y. Frishman and J. Sonnenschein, Phys. Rep. **223** (1993) 309.
- [26] H. U. Yee and I. Zahed, JHEP **1107** (2011) 033 [arXiv:1103.6286 [hep-th]].
- [27] V. Schon and M. Thies, Phys. Rev. D **62** (2000) 096002;
- [28] B. Bringoltz, Phys. Rev. D **79** (2009) 105021; *ibid.* **79** (2009) 125006.
- [29] E. C. Poggio, H. R. Quinn and S. Weinberg, Phys. Rev. D **13**, 1958 (1976).
- [30] L. Y. Glozman, Phys. Rev. D **79**, 037504 (2009) [arXiv:0812.1101 [hep-ph]].
- [31] B. A. Freedman and L. D. McLerran, Phys. Rev. D **16** (1977) 1130; *ibid.* **16** (1977) 1147; *ibid.* **16** (1977) 1169. A. Kurkela, P. Romatschke and A. Vuorinen, Phys. Rev. D **81** (2010) 105021.
- [32] T. K. Herbst, J. M. Pawlowski and B. J. Schaefer, Phys. Lett. B **696**, 58 (2011) [arXiv:1008.0081 [hep-ph]].
- [33] K. Fukushima, Phys. Lett. B **695**, 387 (2011) [arXiv:1006.2596 [hep-ph]].
- [34] S. Lottini and G. Torrieri, arXiv:1103.4824 [nucl-th]; G. Torrieri and I. Mishustin, Phys. Rev. C **82**, 055202 (2010) [arXiv:1006.2471 [nucl-th]].
- [35] S. R. Coleman, Phys. Rev. D **11**, 2088 (1975).
- [36] U. Zuckert, R. Alkofer, H. Weigel and H. Reinhardt, Phys. Rev. C **55** (1997) 2030 [nucl-th/9609012]. L. P. Gamberg, H. Weigel, U. Zuckert and H. Reinhardt, Phys. Rev. D **54** (1996) 5812 [hep-ph/9512294].
- [37] J. -c. Wang, Q. Wang and D. H. Rischke, Phys. Lett. B **704** (2011) 347 [arXiv:1008.4029 [nucl-th]].
- [38] G. S. Adkins, C. R. Nappi and E. Witten, Nucl. Phys. B **228**, 552 (1983).
- [39] S. Weinberg, *The Quantum Theory of Fields, vol.2, Cambridge University Press*.

- [40] O. Schnetz, M. Thies and K. Urlichs, *Annals Phys.* **321** (2006) 2604; G. Basar and G. V. Dunne, *Phys. Rev. Lett.* **100** (2008) 200404; *ibid.* **78** (2008) 065022; *ibid.* **79** (2009) 105012; C. Boehmer and M. Thies, *Phys. Rev. D* **80** (2009) 125038; *ibid.* **81** (2010) 105027.
- [41] C. Vafa and E. Witten, *Nucl. Phys. B* **234** (1984) 173.
- [42] D. Ebert, N. V. Gubina, K. G. Klimenko, S. G. Kurbanov and V. C. Zhukovsky, *Phys. Rev. D* **84** (2011) 025004 [arXiv:1102.4079 [hep-ph]].
- [43] For recent review, M. G. Alford, A. Schmitt, K. Rajagopal and T. Schafer, *Rev. Mod. Phys.* **80**, 1455 (2008) [arXiv:0709.4635 [hep-ph]].
- [44] I. R. Klebanov, *Nucl. Phys. B* **262**, 133 (1985).
- [45] H. Forkel, A. D. Jackson, M. Rho, C. Weiss, A. Wirzba and H. Bang, *Nucl. Phys. B* **504** (1989) 818.
- [46] M. Rho, S. J. Sin and I. Zahed, *Phys. Lett. B* **689** (2010) 23; K. Y. Kim, S. J. Sin and I. Zahed, *J. High Energy Phys.* **001** (2008) 0809; K. Nawa, H. Suganuma and T. Kojo, *Phys. Rev. D* **79**, 026005 (2009) [arXiv:0810.1005 [hep-th]].
- [47] Y. Hidaka, T. Kojo, L. McLerran and R. D. Pisarski, *Nucl. Phys. A* **852**, 155 (2011) [arXiv:1004.2261 [hep-ph]].